

Synthesis of Poly(cyclooctene) by Ring-Opening Metathesis Polymerization: Characterization and Shape Memory Properties

J. Alonso-Villanueva,¹ J. M. Cuevas,² J. M. Laza,¹ J. L. Vilas,¹ L. M. León¹

¹Laboratorio de Química Macromolecular (Labquimac), Universidad del País Vasco (UPV/EHU), 48940 Leioa, Spain

²Gaiker Technological Centre, Parque Tecnológico, Ed. 202, 48170 Zamudio, Spain

Received 23 April 2008; accepted 27 September 2008

DOI 10.1002/app.29394

Published online 15 October 2009 in Wiley InterScience (www.interscience.wiley.com).

ABSTRACT: Cis-cyclooctene was polymerized via ring-opening metathesis polymerization using a well-defined ruthenium catalyst (Grubbs' type) under varying reaction conditions. Control over molecular weight was achieved by the inclusion of a chain transfer agent and its influence on the behavior of the obtained polymers was evaluated. The resulting polymers were characterized by means of differential scanning calorimetry, thermogravimetric analysis, and dynamic mechanical thermal analysis. Taking into account their thermal behavior, samples of appropriate

molecular weight were subjected to a suitable treatment by chemical crosslinking to obtain a material showing thermally induced shape memory effect. The material recovers its original shape after several cycles of deformation into different shapes. © 2009 Wiley Periodicals, Inc. *J Appl Polym Sci* 115:2440–2447, 2010

Key words: polyolefins; ring-opening metathesis polymerization; chain transfer agent; shape memory polymers

INTRODUCTION

Shape memory polymers (SMP) are those capable of recovering their original shape after having been deformed into a different one (temporary shape). In a way, they “remember” the shape they were given when processed (permanent shape) on the basis of entropy changes. Besides, they come back to it several times (deformation cycles), and the temporary shape can be a different one in each case. To do so, these polymers need to be equipped with appropriate molecular structures.¹ There are several SMP based on different structures and functionalities. Various reviews give a good description of the mechanism responsible for the shape memory effect and present quite comprehensive classifications of these materials and their applications.^{2–5}

Most of the SMP reported to date are activated by temperature changes, that is, they are thermally induced shape memory polymers. Another challenging possibility is to activate the shape memory effect by other stimuli. In this sense, light appears as a promising option because it allows activating the

material remotely even at ambient temperature. Some efforts have been made already in this field, and a good control over macromolecular architecture is necessary to place photosensitive groups along the polymer and be able to transfer the movement from the molecular level to the macroscopic world.⁶

At this point is where ring-opening metathesis polymerization (ROMP) may play an interesting role. ROMP is a polymerization technique giving access to that desired control of the polymer structure as well as the preparation of really complicated materials.⁷ This is mainly because of the development of very robust and active initiators that enable the reaction of monomers with different functional groups at mild reaction conditions.^{8–10} To the best of our knowledge, among the polymers synthesized by this technique, only polynorbornene^{11–13} and polycyclooctene¹⁴ have been utilized as SMP so far. We believe that ROMP polymers may go one step further through the inclusion of functional groups that can effectively respond to external stimuli other than heat.

In this contribution, both SMP and ROMP are gathered to obtain a material of controlled molecular weight and having thermally induced shape memory behavior, with a view to extend this study to other kind of stimuli in the future. First, samples of polymer of controlled molecular weight were synthesized by ROMP of *cis*-cyclooctene and the use of Grubbs' second generation catalyst as the initiator.

Correspondence to: L. M. León (luismanuel.leon@ehu.es).

Contract grant sponsor: Spanish Ministerio de Educación y Ciencia; contract grant number: MAT2004-04698-C02-02.

TABLE I
Synthesis of PCO Samples Without CTA

Sample	Monomer: catalyst ratio	Reaction time (min)	Reaction temperature (°C)	Yield (%)	M_n (kg/mol)	PDI
PCO-0	10,000	30	30	84.8	– ^a	– ^a
PCO-1	10,000	60	0	1.5	– ^a	– ^a
PCO-2	10,000	180	0	12.1	– ^a	– ^a
PCO-3	10,000	240	10	53.8	836	1.2
PCO-4	10,000	60	10	20.0	489	1.3
PCO-5	10,000	30	20	81.5	638	1.7
PCO-6	2000	180	0	10.0	448	1.7
PCO-7	500	60	0	–	198	1.9

^a Polymer was insoluble.

Control of the molecular weight was actually quite a demanding task for this particular system. Then, thermal and mechanical properties of the polymer were studied to find the better conditions for processing. Finally, the thermally induced shape memory material was created by thermal crosslinking of the polymer and the shape memory effect was confirmed in a simple experiment.

EXPERIMENTAL

Materials

All reagents used for polymerization, benzylidene[1,3-bis(2,4,6-trimethylphenyl)-4,5-dihydroimidazol-2-ylidene]-dichloro-(tricyclohexylphosphine) ruthenium (second generation Grubbs' catalyst), *cis*-cyclooctene (95%), and *cis*-1,4-diacetoxy-2-butene (95%), were purchased from Aldrich. Dicumyl peroxide was supplied by Merck. Solvents were reagent grade and used without further purification.

Synthesis of polycyclooctene

Polycyclooctene was synthesized by ring-opening metathesis polymerization (ROMP) of *cis*-cyclooctene taking the previously reported method by Mather and coworkers¹⁴ as a reference while introducing some variations regarding the control of the reaction conditions. The experimental procedure used for polymerization is described as follows. First, the

monomer (*cis*-cyclooctene) is dissolved in dichloromethane in a round bottom flask, and the mixture is allowed to stir at the desired temperature under nitrogen atmosphere. The catalyst is then transferred to the reaction flask dissolved in a small quantity of the solvent. After a certain reaction time, some drops of ethyl vinyl ether are added to quench the polymerization. The reaction mixture is then poured into vigorously stirred methanol causing precipitation of a white solid. Methanol is decanted away, and the polymer is reprecipitated twice from chloroform. The reaction conditions are summarized in Table I for the experiments run without control of the molecular weight and in Table II for those in which *cis*-1,4-diacetoxy-2-butene is added as a chain transfer agent (CTA). In these experiments, the CTA is dissolved initially together with the monomer.

After every experiment, the resulting solid is vacuum dried at room temperature until constant weight. Samples are stored under inert atmosphere in the fridge to avoid spontaneous crosslinking.¹⁵

Characterization techniques

Samples were characterized by ¹³C and ¹H-NMR. Spectra were recorded in deuterated chloroform on a Bruker 500 MHz spectrometer. Molecular weights were determined by gel permeation chromatography using a Waters 1515 HPLC isocratic pump and a Waters 2414 refractive index detector, THF as the

TABLE II
Synthesis of PCO Samples in the Presence of *cis*-1,4-Diacetoxy-2-Butene

Sample	Monomer : catalyst ratio	Monomer : CTA ratio	Reaction time (min)	Yield (%)	M_n (kg/mol)	PDI
PCO-8	10,000	40	60	–	48.0	3.0
PCO-9	10,000	40	240	83.0	27.0	1.6
PCO-10	10,000	80	60	94.0	56.8	1.7
PCO-11	10,000	20	60	67.3	24.0	1.7
PCO-12	10,000	60	60	92.7	55.4	1.7
PCO-13	10,000	100	60	87.3	69.1	2.2
PCO-14	10,000	200	60	91.1	103.5	2.4

eluent and a flow rate of 1 mL/min. Polystyrene standards were used for calibration.

Thermal characterization was accomplished by differential scanning calorimetry (DSC) on a Mettler Toledo DSC822^e calorimeter. The samples were subjected to a cyclic dynamic experiment. They were first heated at a rate of 10°C/min from -50 to 150°C; then, the sample was cooled at -10°C/min back to -50°C and heated again to 150°C.

Degradation studies were performed in a thermogravimetric analyzer Mettler Toledo TGA/SDTA 851^e. The samples were first heated from 25 to 50°C at 10°C/min and kept at the final temperature during 20 min to eliminate the remaining humidity. Then they were heated again from 50 to 900°C at a heating rate of 10°C/min. During the process, either an air or nitrogen flow of 50 or 20 mL/min was used, respectively. The products formed during the degradation were analyzed by FT-IR in a Nicolet Nexus spectrometer using a thermogravimetric analysis (TGA) interface connected to a thermogravimetric analyzer Shimadzu DTG-60 and using the same temperature program.

Mechanical properties were measured using a Polymer Laboratories dynamic mechanical thermal analyzer (DMTA) Model Mk II in either bending (dual cantilever geometry) or shear mode with a displacement of 64 μm (strain level $\times 4$). Experiments were dynamic from -100 to 150°C at 2°C/min and three frequencies were measured for all samples 1, 3, and 10 Hz.

Preparation of thermosets

Polycyclooctene (PCO) is dissolved in the minimum amount of CHCl_3 and varying amounts of dicumyl peroxide (weight percent relative to polymer) are added. This solution is allowed to stir for 1 h and then poured onto a Teflon sheet. The solvent is evaporated to form a film, which is later cut into pieces and piled up to fit a metallic mold consisting of bar (bending experiments) and circular shaped (shear experiments) probes. The mold is first compressed at a temperature 10° above the melting temperature and then at 130°C to produce the cured material. In both cases the pressure is set at 200 kg/cm².

RESULTS AND DISCUSSION

Preliminary studies

In our first attempts to obtain PCO, a rapid increase in the viscosity was observed, resulting in total gelation of the reaction mixture within a few minutes from the addition of the initiator. Once the sample was vacuum dried, the polymer was completely in-

soluble. This phenomenon was previously stated by Bielawski and Grubbs¹⁶ when polymerizing cyclooctene in the presence of highly active ruthenium catalyst. However, it is noteworthy that the molecular weight can be measured for some samples which were not completely dried. More specifically, these samples were dried just for over 10 min to eliminate most of the solvent and precipitant. After this treatment, all of them were readily soluble in THF and their molecular distribution could be determined giving quite high molecular weights (Table I). Because the only difference between dried and non-dried samples is the presence of some molecules of solvent separating the polymer chains, the insolubility of dried samples can be attributed to a combination of high molecular weight and high degree of crystallinity¹⁷ that makes them highly stable and prevents redissolution.

Some general characteristics of this ROMP can be drawn from these initial experiments: viscosity can be controlled by lowering the reaction temperature while resulting in lower yields (compare PCO-0 and PCO-1) and in this way, prolonged reaction times are necessary to get a higher yield (PCO-3 and PCO-4). Some attempts were made to lower molecular weight by increasing catalyst loading (see samples PCO-6 and PCO-7) and it was reduced to some extent but samples were still insoluble after complete drying.

Control of the molecular weight

A well-known method for controlling molecular weight in ROMP is through the inclusion of acyclic olefins which effectively act as chain transfer agents (CTAs).¹⁸ In this case, symmetric *cis*-1,4-diacetoxy-2-butene was chosen as the CTA for this system. When this modification is introduced, there is no observable increase in the viscosity of the reaction mixture. In all of the experiments PCO is obtained in relative high yields (even more than 90%), and all of the samples synthesized by this approach are completely soluble in common organic solvents. And what is more important, the molecular weight can be adjusted to the desired applications by varying the monomer to CTA ratio as outlined in Table II. Lower monomer to CTA ratios result in lower molecular weights. PDI is near 2 as expected for this catalyst and in a system in which chain transfer is taking place.^{14,16,19}

The molecular structure is confirmed by ¹³C and ¹H-NMR spectroscopy. Assignments of chemical shifts are consistent with the structure of PCO obtained by other methods.^{20,21} Moreover, as shown in Figure 1, in the ¹H-NMR spectrum two signals can be distinguished in the olefinic region at 5.34 and 5.38 ppm corresponding to *cis* and *trans*

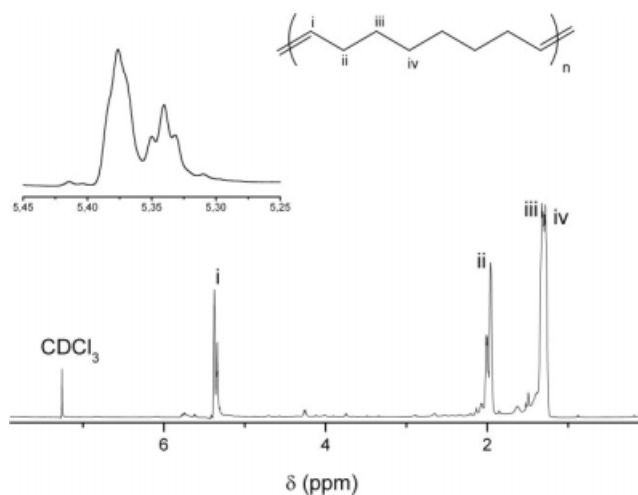


Figure 1 $^1\text{H-NMR}$ spectrum of PCO showing an expanded view of the olefinic region.

insaturations, respectively, although they partially overlap and further analysis would be necessary to establish cis/trans ratio exactly.

Thermal properties and degradation

Polycyclooctene is a semicrystalline thermoplastic as can be drawn from the DSC measurements. In Figure 2 (left), a representative DSC trace of PCO is shown. There is an endothermic peak during the heating step due to the melting of the crystalline areas. After subsequent cooling crystallization is observed as an exothermic peak and the glass transition also appears during the cooling (in the heating the melting peak is too broad and masks it). The melting temperature (T_m) measured in the peak maximum is 46°C . Both crystallization (T_c) and glass transition temperatures (T_g) are determined on the onset of each process. Values of T_c and T_g for this sample are 27 and -23°C , respectively. These temperatures are comparable to other PCO synthesized by other ROMP catalysts.²¹

The thermal history of the PCO samples is decisive. In fact, two important phenomena arise during the first heating step. Firstly, there is an important change in shape between the melting peaks of the first and second heating steps. In the first heating, the peak is broader and even two distinct peaks can be distinguished stemming from varied distribution of sizes and degrees of imperfection of the crystals¹⁷ as well as the microstructure of the polymer (cis and trans microphases).²² In the second heating, there is only one peak which is sharper than before because the different crystals are cooled down from the molten state and crystallize more uniformly at a controlled cooling rate. For this reason, T_m is determined in the second heating step.

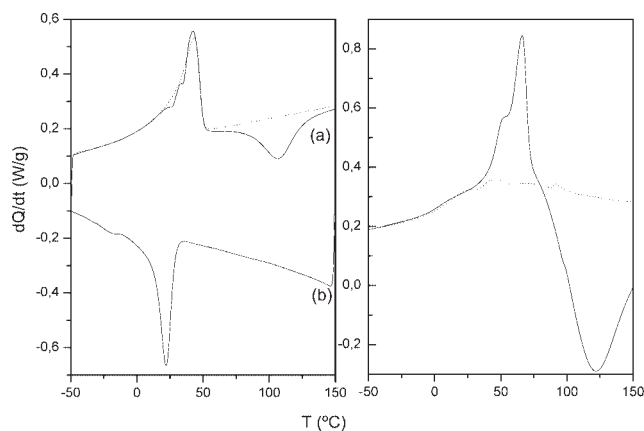


Figure 2 DSC traces of pure PCO. Left, thermal cycle applied to PCO-10: (a) solid line, first heating; (b) cooling; a, dot line) second heating. Right, first heating of uncured PCO-12 (solid line) and after curing in an oven at 125°C for 1 h (dot line).

Secondly, an exothermic peak can be observed at temperatures above 100°C due to partial curing through the reaction of insaturations of nearby chains induced thermally.²³ This point is confirmed by simply curing a sample in an oven at 125°C during 1 h. The result is shown in Figure 2 (right): the uncured sample having the exothermic peak while it is absent in the cured sample. Besides, the degree of crystallinity is reduced almost completely as cross-links would reduce the chain mobility. Surprisingly enough, this thermal crosslinking at quite low temperature takes place only for some of the samples, presumably due to the presence of some kind of impurities in spite of the purifying process through redissolution of the polymers.

After pure PCO has been characterized, dicumyl peroxide is used to cure the polymer in a controlled

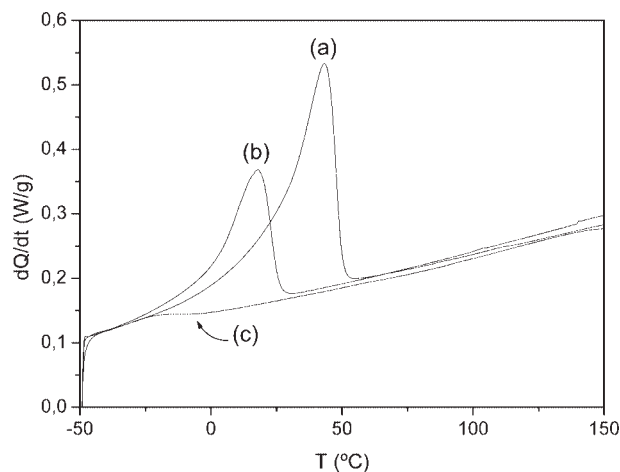


Figure 3 DSC traces of PCO-10 during second heating at a heating rate of $10^\circ\text{C}/\text{min}$: (a) pure PCO; (b) PCO with 3% dicumyl peroxide; and (c) PCO with 7% dicumyl peroxide.

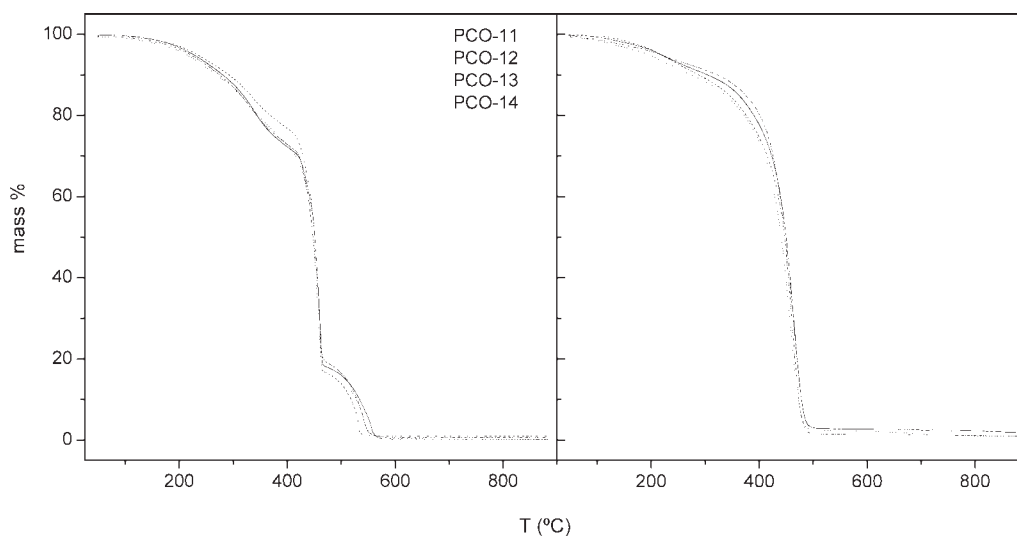


Figure 4 Thermal degradation of various PCO samples under air (left) and nitrogen (right) atmosphere.

manner according to the procedure explained in the experimental part. Peroxide content dramatically affects polymer crystallinity as seen in the DSC measurements. Second heating and cooling steps are presented in Figure 3 for samples of pure PCO and containing 3 and 7 wt % of peroxide. When 3 wt % is used, both the crystallinity degree (related to the area below the melting peak) and T_m decrease. For the sample containing a higher amount of peroxide, the crystalline behavior is completely suppressed and no melting or crystallization peaks are observed.

Four samples of increasing molecular weight were submitted to thermal degradation under air and nitrogen atmosphere (Fig. 4). The initial degradation temperatures (T_i) determined for all the experiments are shown in Table III. During the degradation in air, three degradation steps can be observed. The first one, starting at around 170°C and up to 400°C in which more than 50% of the original mass is retained, is related to the consumption of insaturations which was observed also by DSC measurement. Then, from 400 to 460°C a rapid decrease in the sample mass happens leaving less than 20% of the polymer and finally, as a result of the thermal treatment, the sample is totally degraded, leaving no residue above 570°C. When an inert atmosphere of nitrogen is used, the degradation takes place in a single step for all the samples. In each group of experiments, samples follow the same pattern and there is no clear dependence on the molecular weight as they are only small differences among them.

To get a more detailed study of the degradation process, the sample PCO-11 was submitted to the same thermal treatment and the resulting gases were passed through a FT-IR spectrometer as a function

of time. As can be seen from Figure 5, the main products of degradation in air are carbon dioxide and water as shown by the presence of the typical bands at 2360, 2335 at 670 cm^{-1} for CO_2 and the two groups of bands above 3500 cm^{-1} and between 1900 and 1300 cm^{-1} for H_2O . However, there is also a broad band at 2900 cm^{-1} showing the presence of some hydrocarbon in the spectrum taken at 61 min from the start of the experiment and corresponding to a temperature of 410°C which is located at the middle of the second step of the degradation process. In the experiment under inert atmosphere, the same band appears at different moments of the degradation process corresponding to a hydrocarbon as the only product of degradation at temperatures above 400°C. Unfortunately, in light of the FT-IR spectra an accurate assignment is not possible although a low molecular weight hydrocarbon of 3–5 carbon atoms or a mixture is thought to appear which is in good accordance with previous analysis.²⁴

Therefore, it can be stated that the degradation in air occurs mainly via a thermo-oxidative mechanism combined with a random scission process during the second degradation step while in nitrogen the

TABLE III
Initial Temperatures of Degradation for PCO Samples in Nitrogen and Air Atmosphere

Sample	Nitrogen T_i (°C)	Air T_i (°C)		
		1st step	2nd step	3rd step
PCO-11	416.7	170.7	445.0	515.6
PCO-12	417.5	175.5	448.3	515.6
PCO-13	414.7	177.1	440.8	519.9
PCO-14	422.6	167.6	443.2	515.8

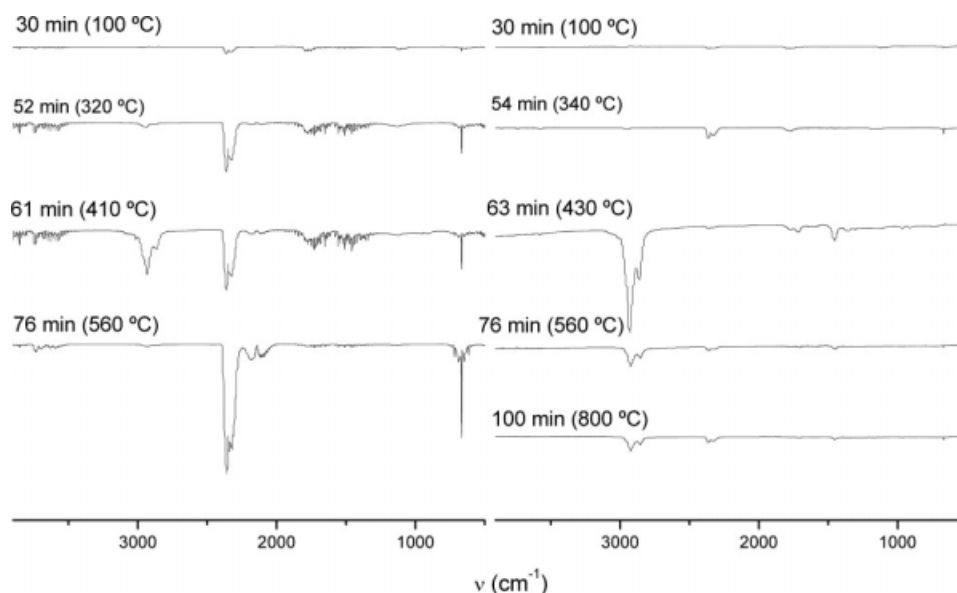


Figure 5 IR spectra of the degradation products of PCO at different times during the thermal degradation process under air (left) and nitrogen (right) atmosphere.

degradation takes place exclusively via random scission of the polymeric chains.

Mechanical analysis

Dynamic mechanical analysis provides valuable information on the mechanical changes in the material as temperature changes. Some DMTA graphics appear in Figure 6 for the sample PCO-10. Neat polymer (Fig. 6, left) having a modulus of 600 MPa at -80°C undergoes a decrease in modulus corresponding to T_g around -40°C . However, there is an abrupt decrease at higher temperatures when the sample begins to melt and after melting takes place, the modulus continues to decrease behaving as a viscous liquid. This is the usual behavior for a thermoplastic that is not useful for shape memory applications as it has no ability to maintain a predetermined shape.

The behavior for cured samples (Fig. 6, right) is different, especially at temperatures above the melting temperature. The value of the storage modulus at low temperature is higher (around 1300 MPa) for samples containing peroxide and cured in the press at 140°C . Glass transition (-45°C) as well as melting occur the same way as for neat PCO, due to the fact that crystallinity is retained in the polymer. In this case, crystalline segments will serve as molecular switches for shape memory actuation. Once the temperature exceeds the melting temperature of the PCO sample, a rubbery plateau is observed. It means that flow is avoided due to crosslinking junctions acting as netpoints. As a result, the shape of the probe is maintained which is decisive for shape memory applications.

Shape memory effect

To evaluate the shape memory capacity of cross-linked PCO samples a simple experiment was carried out. A rectangular bar of PCO-10 with 3% of dicumyl peroxide, the same type of that used for DMTA, was immersed in a hot water bath, stabilized 10°C above the melting temperature of the sample. It soon became soft as the crystallites of the polymer melted while flow was avoided due to the presence of crosslink junctions acting as molecular netpoints. The bar was then deformed into a U shape holding

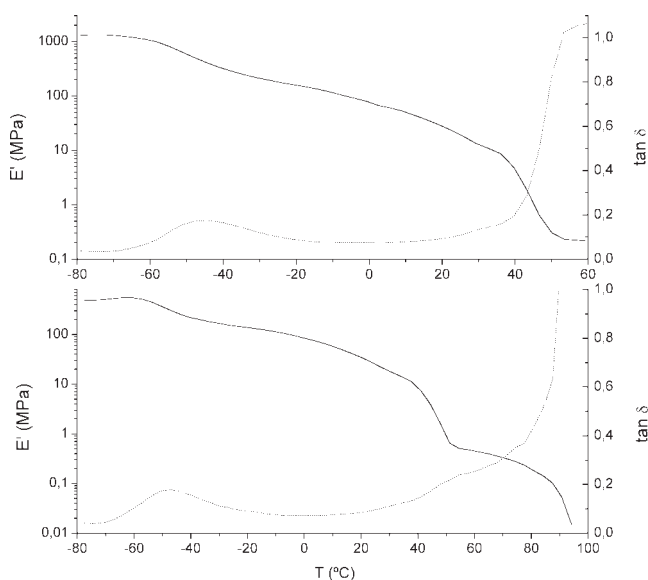


Figure 6 DMTA curves for PCO-10 showing storage modulus (solid line) and $\tan \delta$ (bottom) versus temperature: without peroxide (left); with 3% of dicumyl peroxide (top).



Figure 7 Two sequences of pictures showing shape memory effect for PCO-10 cured with 3% of dicumyl peroxide: first deformation (top) and fourth deformation cycle (bottom).

the bar from the edges with tweezers. This secondary (or temporary) shape was “frozen” by introducing the sample immediately in a cold water bath (ice/water). This process is known as the programming step of the shape memory polymer.

When the sample was immersed again in the hot water bath (Fig. 7, top), complete and fast recovery of the permanent (or primary) shape was observed. The melting temperature acts as the limiting temperature for shape memory actuation, meaning that it is necessary to surpass it so as to program and activate again the shape memory effect. The process of programming and activation by this method could be repeated several times, so it was possible to establish a cycle of shape memory behavior for this polymer. In fact, different temporary shapes are possible in each cycle, although recovery was found to be incomplete after the third cycle (Fig. 7, bottom).

CONCLUSIONS

ROMP has been used as the synthetic route to obtain a thermally induced shape memory polymer using *cis*-cyclooctene as the monomer and second generation Grubbs’ catalyst as initiator. The reaction in solution was very fast and uncontrollable even at low temperature or monomer concentration, and polymers obtained in this way are insoluble after complete drying. It was found that 1,4-diacetoxy-2-butene acts preventing gelation and allowing control of the molecular weight. To lower molecular weight of the samples, higher amounts of this agent need to be added with respect to the monomer.

Poly(cyclooctene) thus obtained is a semicrystalline polymer with a melting temperature at around 40°C and thermal degradation of the insaturations is found for some samples after heating above 100°C. Even in that case, crystallization and melting occur and are not affected as seen after repeated cooling and heating by DSC. Degradation of the polymeric chains takes place at around 430°C both in thermooxidative and inert atmosphere producing low molecular weight hydrocarbons.

Crosslinking of the synthesized polymer has been achieved by addition of dicumyl peroxide and subsequent heating although a high degree of crosslinking will diminish the crystalline behavior. A shape memory specimen has been produced by this method and its shape memory effect has been proved using the melting temperature of the material as the switching temperature. The cycle of deformation and activation can be repeated several times.

Although this is a thermally triggered shape memory polymer, we believe we managed to get a better control of the ROMP process for the future modification of the polymer structure and activation of the shape memory effect by other stimuli.

References

1. Behl, M.; Lendlein, A. *Mater Today* 2007, 10, 20.
2. Lendlein, A.; Kelch, S. *Angew Chem Int Ed* 2002, 41, 2034.
3. Liu, C.; Qin, H.; Mather, P. T. *J Mater Chem* 2007, 17, 1543.
4. Lendlein, A. *Smart Fibres, Fabrics and Clothing*; Woodhead Publishing: Cambridge, 2001, p 278.
5. El Feninat, F.; Laroche, G.; Fiset, M.; Mantovani, D. *Adv Eng Mater* 2002, 4, 91.
6. Jiang, H.; Kelch, S.; Lendlein, A. *Adv Mater* 2006, 18, 1471.

7. Grubbs, R.H., Ed. Handbook of Metathesis, Vol. 1; Wiley-VCH: Weinheim, 2003.
8. Trnka, T. M.; Grubbs, R. H. *Acc Chem Res* 2001, 34, 18.
9. Buchmeiser, M. R. *Chem Rev* 2000, 100, 1565.
10. Slugovc C. *Macromol Rapid Commun* 2004, 25, 1283.
11. Yamamoto, E. *Purasuchikkusu* 1987, 38, 107.
12. Nagata, N. *Kagaka* 1990, 45, 554.
13. Jeon, H. G.; Mather, P. T.; Haddad, T. S. *Polym Int* 200, 49, 453.
14. Liu, C.; Chung, S. B.; Mather, P. T.; Zheng, L.; Haley, E. H.; Coughlin, E. B. *Macromolecules* 2002, 35, 9868.
15. Morel, M.; Lacoste, J.; Baba, M. *Polymer* 2005, 46, 9274.
16. Bielawski, C. W.; Grubbs, R. H. *Angew Chem Int Ed* 2000, 39, 2903.
17. Schneider, W. A.; Müller, F. *J Mol Catal* 1988, 46, 395.
18. Bielawski, C. W.; Benitez, D.; Morita, T.; Grubbs, R. H. *Macromolecules* 2001, 34, 8610.
19. Sanford, M. S.; Love, J. A.; Grubbs, R. H. *J Am Chem Soc* 2001, 123, 6543.
20. Dounis, P.; Feast, W. J.; Kenwright, A. M. *Polymer* 1995, 36, 2787.
21. Çetinkaya, S.; Karabulut, S.; Düz, B.; İmamoglu, Y. *Appl Organomet Chem* 2005, 19, 347.
22. Commereuc, S.; Svecova, L.; Verney, V. *Macromol Chem Phys* 2003, 204, 76.
23. Giurginca, M.; Zaharescu, T. *Polym Degrad Stab* 2002, 75, 267.
24. Mühlebach, A.; van der Schaaf, P. A.; Hafner, A.; Setiabudi, F. *J Mol Catal A* 1998, 132, 181.